Colloids and Surfaces A 558 (2018) 144–153

Contents lists available at ScienceDirect

Colloids and Surfaces A

journal homepage: www.elsevier.com/locate/colsurfa

Hybrid polysaccharide beads for enhancing adsorption of Cr(VI) ions

Gabriel G. Arantes de Carvalho[a], Gislayne A.R. Kelmer[a], Pedro Fardim[b], Pedro V. Oliveira[a], Denise F.S. Petri[a,*]

[a] Department of Fundamental Chemistry, Institute of Chemistry, University of São Paulo, Av. Prof. Lineu Prestes 748, 05508-000, São Paulo, Brazil
[b] Department of Chemical Engineering, University of Leuven, Celestijnenlaan 200F, 3001 Leuven, Belgium

GRAPHICAL ABSTRACT

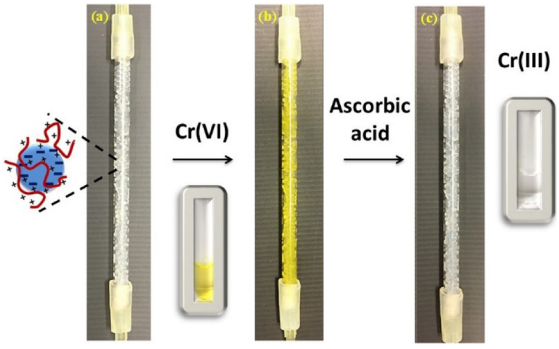

ARTICLE INFO

Keywords:
Alginate beads
Poly(4-vinyl-*N*-pentyl pyridinium bromide)
Cr(VI)
Adsorption
Ascorbic acid

ABSTRACT

Alginate (Alg) beads were modified by the adsorption of poly(4-vinyl-*N*-pentyl pyridinium bromide (QVPV) polycation, aiming towards the adsorption of Cr(VI) ions from aqueous solution. The adsorption isotherm of QPVP onto Alg beads fitted well the Langmuir adsorption model, yielding maximum adsorption capacity (q_{max}) of 91 mg g^{-1} and high constant affinity of 7.53×10^7 L mol^{-1}. X-ray photoelectron spectroscopy and elemental analysis indicated that the QPVP chains were mainly on the Alg beads surface. The adsorption of Cr(VI) in the dilute range (0.5 mg L^{-1} to 10 mg L^{-1}) on Alg-QPVP beads in batch system was investigated by means of flame atomic absorption spectrometry. Under optimal adsorption conditions (HNO_3, pH 2, 6 mg of dried beads, 15 mL of solution, 30 min contact time) the nonlinear fitting with Langmuir model yielded q_{max} of 18 mg g^{-1} and constant affinity of 124 L mol^{-1}, whereas the q_{max} of 156 mg g^{-1} and adsorption energy of 9.8 kJ mol^{-1} were obtained from linear fitting with Dubinin-Radushkevitch model. The breakthrough curves obtained for Cr(VI) at 100 mg L^{-1} in the fixed bed column system were fitted to the Adams-Bohart and Thomas models. Fitting parameters indicated a fast dynamic adsorption process, which takes place mainly on the beads surface. The reduction of adsorbed Cr(VI) ions to Cr(III) by ascorbic acid, a non-toxic biological reductant, allowed the fast and complete recycling of the Alg-QPVP beads for at least 20 times without losing performance. Novel Alg-QPVP beads presented attractive features for dynamic process, such as quickness ($k > 1 \times 10^{-3}$ L mg^{-1} min^{-1}) and high adsorption capacity in the dilute range, low cost and recycling possibility.

* Corresponding author.
E-mail address: dfsp@iq.usp.br (D.F.S. Petri).

https://doi.org/10.1016/j.colsurfa.2018.08.053
Received 12 July 2018; Received in revised form 23 August 2018; Accepted 24 August 2018
Available online 25 August 2018
0927-7757/

1. Introduction

Water is essential for human survival and crucial for life on Earth. Water resources are random distributed in space and time. Human activities generate organic and inorganic residues, which are disposed in wastewater that must be treated in order to be re-used and to avoid the contamination of ground water, rivers and oceans. The treatment depends on the type of contaminant; in the case of inorganics, the most common techniques are coagulation followed by precipitation, adsorption, reverse osmosis, electrodialysis membrane separation and bioremediation [1]. Among all methods, adsorption on recyclable and natural substrates is one of the most advantageous technique because the adsorbents are cost efficient, they do not require high-energy consumption, they do not generate toxic sub-products, and most of the time can be regenerated after the adsorption cycle [2]. Polysaccharides are interesting materials for the development of new adsorbents because they are biodegradable, and they stem from renewable sources, causing low environmental impact. Sodium alginate (Alg) is a natural linear anionic polysaccharide extracted from algae cell wall. Alg chains are composed of (1–4) β-linked D-mannuronic acid (M) and (1–4) α linked L-guluronic acid (G) blocks. In the presence of divalent cations, such as calcium ions, the G–G sequences form complexes with the divalent cations, the so-called 'egg box junctions [3], leading to stable beads. Alg beads proved to be very efficient in the uptake of potentially toxic elements such as Pb, Cd and Cu [4], and rare earth elements [5,6]. At pH higher than 4 the M and G blocks are deprotonated and can bind to positively charged ions by means of electrostatic interactions. However, Alg beads are not efficient for the removal of anionic metallic ions, such as chromate or dichromate ions, due to electrostatic repulsion.

The trivalent and hexavalent chromium, Cr(III) and Cr(VI), ions are among the most common potentially toxic elements found in wastewater. Cr(III), positively charged, is an essential micronutrient for normal energy metabolism of humans. On the other hand, Cr(VI), found as chromate or dichromate anions, might cause severe health problems such as carcinogenesis, liver and kidney failure [7,8]. In order to adsorb Cr(VI) by electrostatic interaction the adsorbent should be positively charged. For instance, hybrid membranes of chitosan/carboxylmethyl cellulose/silica presented adsorption capacity of ~ 20 mg g^{-1} Cr(VI) at pH between 1 and 2; at this pH chitosan amine groups were protonated and attracted dichromate ions [9]. Ethylenediamine-modified cross-linked magnetic chitosan resin displayed adsorption capacity of 51.8 mg g^{-1} Cr(VI) [10]. The maximum adsorption capacity of Cr(VI) on chitosan/polycaprolactam nanofibrous filter paper via filtration amounted to 114.7 mg g^{-1} [11]. Recently, alginate beads were chemically modified by the attachment of polyethylenimine (PEI) mediated by glutaraldehyde; at pH 2 the amine groups became protonated and maximum adsorption capacity achieved the level of 431.6 mg g^{-1} Cr (VI) [12]. Highly porous alginate beads modified by polydopamine and PEI showed the excellent adsorption capacity of 524.7 mg g^{-1} Cr(VI) [13]. Carbodiimide mediated the modification of carboxylated cellulose nanocrystals by PEI, yielding adsorbents with adsorption capacity of 358.4 mg g^{-1} Cr(VI) [14]. Amine functionalities were chemically introduced on corn stalks [15,16] to create attractive sorbents for Cr(VI).

In the present study, we present a novel adsorbent for Cr(VI) composed of Alg beads, which were modified by the adsorption of poly(4-vinyl-*N*-pentylpyridinium bromide), QPVP, an outstanding antimicrobial polycation [17,18]. The Alg-QPVP beads were characterized by means of Fourier transform infrared (FTIR) spectroscopy, scanning electron microscopy (SEM), X-ray photoelectron spectroscopy (XPS) and elemental analysis (CHN). The maximum contaminant level of Cr(VI) in drinking water was set as 0.1 mg L^{-1} by the NSF International agency (http://www.nsf.org/consumer-resources/water-quality/water-filters-testing-treatment/contaminant-testing-procedures). Thus it is very important to develop adsorbents and experimental conditions that efficiently separate low amounts of Cr(VI) in aqueous media. For this reason, the adsorption behavior of Cr(VI) onto Alg-QPVP beads was investigated in batch system and detected by flame atomic absorption spectrometry (FAAS). The relevant parameters, such as type of acid used to adjust the pH, medium pH for adsorption, mass of adsorbent and contact time, were systematically investigated. Additionally, for practical purposes, the adsorption of Cr(VI) on Alg-QPVP beads was conducted using a fixed bed column system under optimal conditions. The possibility of adsorbent recycling was evaluated by the reduction of adsorbed Cr(VI) to Cr(III) by ascorbic acid (vitamin C), a non-toxic biological reductant, allowing a quantitative desorption of all chromium of the Alg-QPVP beads.

2. Experimental

2.1. Materials

Alginic acid sodium salt (180947, mannuronate/guluronate ratio = 1.56, M_w from 120,000 g mol^{-1} to 190,000 g mol^{-1}), poly(4-vinylpyridine) (PVP) (472344, $\overline{M_w}$ 60,000 g mol^{-1}, degree of polymerization ~566) and 1-bromopenthane (purity 99%) were purchased from Sigma-Aldrich (Brazil). $CaCl_2$, anhydrous ethanol (98%), diethyl ether (99%) and HBr (48%) were provided by Labsynth (Sao Paulo, Brazil). Standard solutions from Titrisol® containing 1000 mg L^{-1} Cr (VI) ($K_2Cr_2O_7$) (Merck, Darmstadt, Germany) were used as chromium species for adsorption tests. Hydrochloric, nitric, sulfuric and orthophosphoric acids (Merck, Darmstadt, Germany) were used for pH adjustment or to investigate the influence of acid type onto the adsorption. Ascorbic acid ($C_6H_8O_6$) (Vetec, Brazil) was used for desorption of Cr(VI) from Alg-QPVP.

2.2. Synthesis and characterization of poly(4-vinyl-N-pentyl pyridinium bromide) (QPVP)

Poly(4-vinyl-*N*-pentyl pyridinium bromide) (QPVP) was synthesized as described elsewhere [18]. Briefly, PVP (10 wt%) was dissolved in anhydrous ethanol in a flask with a reflux condenser. 1-bromopentane was added (excess of 5 times the stoichiometric amount) and mixture was stirred under N_2 atmosphere for 24 h, at 60 °C. The reaction is presented in the Supplementary Material Figure SM1. The mixture was then precipitated in diethyl ether to obtain a slightly yellow solid that was re-dissolved in ethanol and re-precipitated the same way. The product was washed with a cold 0.1 mol L^{-1} HBr solution in order to remove any eventual unreacted molecules, washed with diethyl ether once more, and dried under vacuum at room temperature.

KBr pellets containing QPVP powder were prepared for FTIR spectroscopy analyses with a Perkin Elmer Frontier equipment, with resolution of 4 cm^{-1}, in the range of 600 cm^{-1} to 4000 cm^{-1}. The effectiveness of the quaternization was evaluated by the disappearance of the band at 1600 cm^{-1}, which is characteristic of pyridine N − C stretching, and the appearance of a band at 1640 cm^{-1}, which is typical for pyridinium cations.

2.3. Preparation of alginate beads modified with QPVP

First, alginate (Alg) beads were prepared by dissolving alginic acid sodium salt in distilled water at 3% (w v^{-1}), under constant stirring at 24 ± 1 °C, for 1 h. Then the solution was added drop wise with a burette into 150 mL of $CaCl_2$ solution at 4% (w v^{-1}), under constant stirring at 24 ± 1 °C, resulting in instantaneous formation of spherical beads due to electrostatic interactions between guluronate blocks and Ca^{2+}. The synthetized beads were kept in the $CaCl_2$ solution for a period of 10 min to facilitate the diffusion of Ca^{2+} ions into the polymeric beads, which will further increase their stability. The beads were then removed from the $CaCl_2$ solution by means of a plastic 400–500 μm mesh sieve and washed with Milli-Q water until the conductivity achieved ~ 10 μS cm^{-1} at 24 ± 1 °C.

The adsorption isotherm of QPVP onto Alg beads was obtained at 24 ± 1 °C and pH 5.5, in the QPVP concentration range of 0.05 g L^{-1} to

2.0 g L^{-1}. The mass of dried beads and the QPVP solution volume were kept constant as ~ 50 mg and 2 mL, respectively. Alg beads and QPVP interacted for 1 h under constant rotation at 3 rpm in a homemade vertical carrousel (Supplementary Material SM1). The adsorption time of 1 h was enough to assure equilibrium conditions; longer contact times did not increase the adsorption of QPVP on Alg beads. Then the systems were centrifuged at 2000 rpm for 10 min, and their supernatants were separated from the beads. The concentration of free QPVP in the supernatants was determined by UV–Vis spectrophotometry at 256 nm in a Beckman-Coulter DU640 spectrophotometer (Supplementary Material Figure SM2). The concentration of adsorbed QPVP onto the particles was determined as the difference between the initial concentration (C_0) of QPVP and the QPVP concentration in the supernatants, or the equilibrium concentration (C_e). The equilibrium adsorption capacity (q_e, mg g^{-1}) of QPVP was calculated dividing the concentration of adsorbed QPVP by the mass of dried beads (m) and multiplying by the solution volume (v):

$$q_e = \frac{C_0 - C_e}{m} \times v \quad (1)$$

The QPVP coated beads, coded as Alg-QPVP, were rinsed with Milli-Q water until the conductivity achieved ~ 10 μS cm^{-1} at 24 ± 1 °C.

2.4. Characterization of Alg and Alg-QPVP beads

Alg and Alg-QPVP beads were dried in the oven at 40 ± 1 °C overnight and characterized. FTIR spectra of ground Alg and Alg-QPVP beads were obtained with KBr pellets (5 mg samples per 200 mg KBr, thickness 1 mm). SEM analyses were performed in a Jeol Neoscope microscope JCM 5000, operating at 5 kV. The samples were coated with a thin (~ 2 nm) gold layer prior to the analyses. XPS measurements were performed in freeze-dried beads with a Physical Electronics PHI Quantum 2000 PS instrument equipped with monochromatic Al Kα X-ray source. Three different spots were analyzed on each sample. Photoelectrons were collected using electrons detector with the pass energy of 187 eV, step size 1.6 eV, in low-resolution survey mode, and 46.95 eV, step size 0.4 eV, in high-resolution mode C1s. Elemental analyses of dried Alg-QPVP beads were performed using a PerkinElmer 2400 CHN Elemental Analyzer for the determination of C, H and N.

2.5. Adsorption isotherm of Cr(VI) onto cationic Alg-QPVP beads

A model AAS Vario 6 flame atomic absorption spectrometer (Analytik JenaAG, Jena, Germany) was used for the determination of Cr in aqueous solutions. The determinations of Cr were done using a hallow cathode lamp with current of 5.0 mA, wavelength of 357.9 nm and resolution of 0.2 nm.

In order to evaluate the performance of the cationic bead on Cr(VI) adsorption efficiency, different parameters were studied, such as type of acid medium (HCl, HNO_3, H_2SO_4 and H_3PO_4) for standard solution preparation, pH (from 2 to 9), contact time between Alg-QPVP bead and Cr(VI) solution (from 1 to 240 min), mass of wet adsorbent (from 50 to 1000 mg), and Cr(VI) concentration (from 0.5–10 mg L^{-1}). One should notice that 1 g of dried Alg-QPVP beads sucked 32 g of water or acid medium under equilibrium conditions. The optimization experiments were carried out in batch system in order to define the most appropriate physical and chemical conditions for the Cr(VI) adsorption on cationic beads.

Removal efficiency (Q) of analyte from aqueous solution by the beads was calculated through the following expression:

$$Q\ (\%) = \frac{C_0 - C_s}{C_0} \times 100 \quad (2)$$

where C_0 is the initial concentration of analyte in the aqueous solution and C_s is the concentration of analyte in the supernatant after adsorption.

In order to verify the influence of different acid medium on the Cr (VI) adsorption, 400 mg of wet Alg-QPVP beads were added to 15 mL of Cr(VI) solution at 1 mg L^{-1} prepared in HCl, HNO_3, H_2SO_4 or H_3PO_4, maintaining pH 2. After shaking for 30 min in a horizontal rotary shaker at 300 rpm, the supernatant was separated from the Alg-QPVP beads and the remaining Cr(VI) in solution was determined by FAAS.

The effect of pH (from 2 to 9) on Cr(VI) adsorption efficiency was investigated using 400 mg of wet Alg-QPVP beads in contact with 15 mL of 1 mg L^{-1} Cr(VI) standard solution. After 30 min shaking at 300 rpm, the supernatant was separated and analyzed by FAAS. The influence of contact time was evaluated with 400 mg of wet Alg-QPVP beads in contact with 15 mL of 1 mg L^{-1} Cr(VI) standard solution in HNO_3 medium, at pH 2, stirring at 300 rpm; the contact time varied from 15 min to 4 h. The effect of the adsorbents mass (from 50 to 1000 mg wet basis) was also evaluated with 15 mL of 1 mg L^{-1} Cr(VI), shaking for 30 min (300 rpm). Adsorption isotherm of Cr(VI) on Alg-QPVP beads was determined in the concentration range of 0.5 to 10 mg L^{-1} in HNO_3 medium, at pH 2 and 24 ± 1 °C, stirring at 300 rpm. The mass of wet Alg-QPVP beads of 200 mg (i.e., ~ 6 mg dry basis) and the solution volume of 15 mL were kept constant for all experiments.

2.6. Adsorption experiments in a fixed-bed column

Continuous flow adsorption experiments were conducted in a fixed bed glass column with inner diameter of 6 mm, height of 12 cm, assembled with glass wool at the bottom and upper ends. Silicone sleeves and pipette tips were used to couple the column to silicone Tygon® tubes attached to a peristaltic pump (Ismatec, Switzerland). All experiments were performed at constant flow rate of 0.5 mL min^{-1}. The fixed bed column was packed with 2 g of wet Alg-QPVP beads (i.e., ~60 mg dry basis; bed depth of 12 cm). Breakthrough curves were built by determining the Cr(VI) concentration (C_t) in aliquots of eluate collected in time intervals of one minute. The initial concentration (C_0) of Cr(VI) ion solution was 10 mg L^{-1} or 100 mg L^{-1}, prepared at pH 1. In order to promote desorption of Cr(VI), a 0.2% (w v^{-1}) ascorbic acid in 0.1 mol L^{-1} HCl solution was loaded in the reverse direction, at flow rate of 0.5 mL min^{-1}. The concentration of Cr in the eluate was determined in defined time intervals by FAAS, in order to determine the desorbed amount as a function of time.

In order to evaluate the column reusability, cycles of adsorption-desorption were also performed with initial concentration (C_0) of Cr(VI) ion solution of 100 mg L^{-1}, prepared at pH 1, which was loaded into the Alg-QPVP beads column at 0.5 mL min^{-1} flow rate. In order to promote desorption of Cr(VI), 2 mL of a 0.2% (w v^{-1}) ascorbic acid in 0.1 mol L^{-1} HCl solution was loaded in the reverse direction, at flow rate of 0.5 mL min^{-1}. Then, the column was rinsed and conditioned by loading 2 mL of a 0.1 mol L^{-1} HNO_3 prior to the next run.

3. Results and discussion

3.1. Adsorption of QPVP on Alg beads

The FTIR spectra determined for PVP and QPVP (Supplementary Material Figure SM3) evidenced qualitatively the efficient quaternization of PVP. CHN analyses (PerkinElmer 2400 CHN Elemental Analyzer) indicated the quaternization efficiency of 82%, increasing the average molecular weight of QPVP chains to 126,000 g mol^{-1}. Fig. 1 shows the adsorption isotherm of QPVP on Alg beads at (24 ± 1) °C and pH 5.5, along with the nonlinear fittings with the two-parameters adsorption models of Langmuir, Freundlich and Dubinin-Radushkevitch (D–R) [19,20]. The fittings with the linearized equations of Langmuir, Freundlich and D–R adsorption models are available as Supplementary Material SM4. The equations and the linearized forms corresponding to each adsorption model are presented in Table 1.

Table 2 comprises the parameters resulting from nonlinear and linear fittings. Following the literature recommendation [20], in order

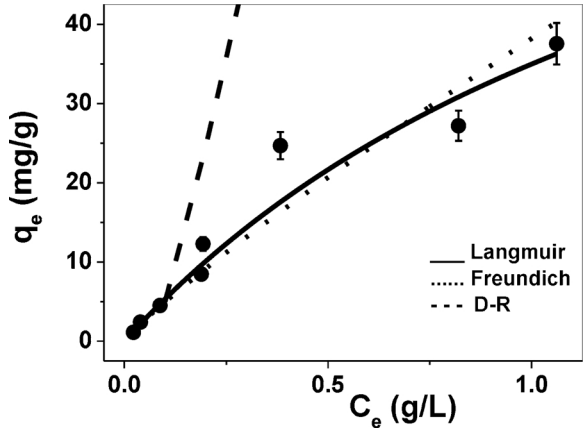

Fig. 1. Adsorption isotherm of QPVP on Alginate beads at 24 ± 1 °C and pH 5.5, along with nonlinear fitting for Langmuir, Freundlich and D–R models.

to identify the best model, one should compare the chi-squared (χ^2) values obtained from the nonlinear fittings in addition to the correlation coefficient determined from the linear fittings (R^2), which can be calculated by Eqs. (3) and (4), respectively. The criteria for the best fitting are the smallest χ^2 value and the R^2 value closest to 1.

$$\chi^2 = \sum \frac{(q_{e,exp} - q_{e,calc})^2}{q_{e,calc}} \quad (3)$$

$$R^2 = 1 - \frac{\sum (q_{e,exp} - q_{e,calc})^2}{\sum (q_{e,exp} - q_{e,mean})^2} \quad (4)$$

Table 2 shows the fitting parameters determined from each model, along with the χ^2 and R^2 values. The nonlinear fittings indicated the Langmuir model as the best one because it yielded the lowest χ^2 values; the q_{max} and K_L values amounted to 91 mg g^{-1} and 0.625 L mg^{-1}, respectively. Although the linear fitting of experimental data to Langmuir model yielded R^2 value of 0.5702, the fitting parameters from nonlinear and linear fittings converged to similar q_{max} and K_L values. The K_L value of 0.625 L mg^{-1} (or 7.53×10^7 L mol^{-1}) indicates the high affinity among QPVP chains and Alg beads. The nonlinear and linear fittings obtained with Freundlich model also resulted in similar n and K_F values. The nonlinear fitting with D–R model converged just in the low C_e range (up to 0.2 g L^{-1}), yielding q_{max} of 187 mg g^{-1} and E of 2.2 kJ mol^{-1}. On the hand, the linear fit presented q_{max} and E values of 3754 mg g^{-1} and 9.6 kJ mol^{-1}, which are much larger than those determined from the nonlinear fitting. Considering the electrostatic interactions among QPVP cationic chains and Alg carboxylate groups, the E value of 9.6 kJ mol^{-1} determined from linear fitting with D–R model is more reasonable than the E value of 2.2 kJ mol^{-1} determined from nonlinear fitting.

The isotherm in Fig. 1 showed experimental q_e values smaller than the calculated q_{max} values determined by the nonlinear fitting with Langmuir or D–R models, indicating that under those experimental conditions QPVP chains occupied only a fraction of bead surface. One plausible reason for this is that, at the adsorption initial stages, all M blocks carboxylate groups are free to bind to the charged segments of QPVP chains. They probably do not adsorb flat on the surface, but instead, part of the chains might dangle in solution building a cationic layer around the beads. Under equilibrium conditions, such cationic layer repels the approaching QPVP chains by electrostatic repulsion, impairing a uniform surface modification.

After adsorption of QPVP, the beads were withdrawn from solution and immersed into 2 mL distilled water in order to evaluate the possibility of QPVP desorption. After 24 h the supernatant was analyzed and the concentration of QPVP was below the limit of detection (< 0.1 mg L^{-1}) of the UV–vis spectrophotometer, indicating QPVP desorption was negligible.

The FTIR spectra (Fig. 2a) of dried Alg and Alg-QPVP (q_e = 38 mg g^{-1}) beads both showed the bands at 3440, 1620, 1415, and 1031 cm^{-1}, attributed to the stretching of O—H, C═O (acid groups), CH— (bending), and C—O—C, respectively, which are typical from alginate matrix. The spectra of Alg-QPVP beads showed the bands at 1641, 1517 and 1467 cm^{-1}, which are attributed to pyridinium C–N (stretching) and aromatic ring C═C (stretching), respectively, and are not present in the alginate spectrum (Fig. 2b). Such features evidenced the adsorption of QPVP onto Alg beads.

The CHN elemental analyses performed for dried Alg-QPVP (q_e = 38 mg g^{-1}) indicated C and N contents of 35.3 ± 0.3% and 1.70 ± 0.05%, respectively; the ratio C/N amounted to 20.76. XPS analyses performed for Alg and Alg-QPVP yielded the contents of C, O, N and Ca on the beads surface (~ 7 nm of depth), as shown in Table 3. The content of 4% N and the ratio C/N of 18.52 were determined for Alg-QPVP beads. The similarity in the C/N ratios observed from CHN and XPS measurements indicated that most QPVP chains are on the Alg beads surface.

The modification of Alg beads with QPVP led to substantial changes

Table 1
Equations and the corresponding linearized forms of Langmuir, Freundlich and Dubinin-Radushkevitch (D–R) adsorption models. C_e, q_e and q_{max} stand for equilibrium concentration (mg L^{-1}), adsorption at equilibrium (mg g^{-1}) and maximum adsorption, respectively [19,20].

Model	Equation
Langmuir	$q_e = \frac{q_{max} K_L}{1 + K_L C_e}$
	K_L = *adsorption equilibrium constant*
	Linearized form: $\frac{C_e}{q_e} = \frac{C_e}{q_{max}} + \frac{1}{q_{max} K_L}$
	Plot: $\frac{C_e}{q_e}$ as a function of C_e
Freundlich	$q_e = K_F C_e$
	K_L = *Freundlich constant, the larger KF, the higher the adsorption capacity*
	n is related to the surface heterogeneity, the smaller n, the greater the heterogeneity.
	Linearized form: $\ln q_e = \ln K_F + \frac{1}{n} \ln C_e$
	Plot: $\ln q_e$ as a function of $\ln C_e$
D-R	$q_e = q_{max} e^{-\beta \varepsilon^2}$
	$\varepsilon = RTln\left[1 + \frac{1}{C_e}\right]$ (J mol^{-1}) = the Polanyi potential, R is the gas constant (8.314 J mol^{-1} K^{-1}) and T is temperature
	Linearized form: $\ln q_e = \ln q_{max} - \beta \varepsilon^2$
	Plot: $\ln q_e$ as a function of ε^2
	$E = \frac{1}{\sqrt{2\beta}}$, E = mean free energy of adsorption (kJ mol^{-1})

Table 2
Adsorption of QPVP onto alginate beads. Parameters determined from nonlinear and linear fittings corresponding to each model, along with the χ^2 and R^2 values.

Nonlinear fitting		
Langmuir	Freundlich	D-R
q_{max} = 91 mg g^{-1} K_L = 0.625 L mg^{-1}	n = 0.8856 $K_F = 38.20 \left(\frac{mg}{L \times g}\right) / \left(\frac{mg}{L \times g}\right)^{\frac{1}{n}}$	q_{max} = 187 mg g^{-1} E = 2.2 kJ mol^{-1}
χ^2 = 6.266	χ^2 = 9.053	χ^2 = 12.3
Linear fitting		
Langmuir	Freundlich	D-R
q_{max} = 87 mg g^{-1} K_L = 0.6812 L mg^{-1}	n = 0.8961 $K_F = 41.02 \left(\frac{mg}{L \times g}\right) / \left(\frac{mg}{L \times g}\right)^{\frac{1}{n}}$	q_{max} = 3754 mg g^{-1} E = 9.6 kJ mol^{-1}
R^2 = 0.5702	R^2 = 0.9662	R^2 = 0.9746

in the morphological characteristics of the beads' surface. SEM images revealed the smooth surface of Alg beads, which turned rough after QPVP adsorption (Fig. 3a,c). The photographs of wet Alg and Alg-QPVP beads showed that after QPVP adsorption the beads became yellowish (Fig. 3b,d). Alg-QPVP remained over one year in water without losing form and biodecomposition; QPVP is well known for its antimicrobial activity [17,18]. On the other hand, Alg beads cannot be stored in water for longer than two weeks due to the growth of microorganisms.

3.2. Adsorption of Cr(VI) onto cationic Alg-QPVP beads in batch system

Fig. 4 shows the solutions for each different acid media, after the interaction with Alg-QPVP beads. Except for the HNO_3, the formation of foam could be observed after contact with HCl, H_2SO_4 and H_3PO_4; it is probably due to the leaching of QPVP, which has surfactant properties [21]. Ions such as sulfate, phosphate and, to a lesser extent, chloride, might cause "salting-out" effect on macromolecules, causing the QPVP desorption from the alginate beads. For this reason, all adsorption experiments were performed in HNO_3 media.

The influence of pH (from 2 to 9) on Cr(VI) adsorption efficiency was investigated using 400 mg of wet Alg-QPVP beads in contact with 15 mL of 1 mg L^{-1} Cr(VI) solution. After 30 min shaking, the supernatant was separated and analyzed by FAAS. The highest adsorption efficiency of Cr(VI) ($Q \sim 60\%$) was attained at pH 2 (HNO_3 solution), corroborating with literature reports [9,12,15].

Fig. 5a shows the dependence of the contact time on the Q values. Already after 15 min the Q value achieved 54% and practically did not change for longer adsorption time (4 h), when Q value achieved 58%. Such relatively fast adsorption process is due to strong electrostatic interaction among the positively charged Alg-QPVP surface and dichromate anions. Fig. 5b shows the effect of the mass of wet Alg-QPVP beads on the Q values. The minimal amount of wet bead necessary to reach 48% retention of Cr(VI) was 200 mg. Larger amounts led to a small increase of Q to 55%. Fig. 5c shows the Cr(VI) adsorption isotherm on Alg-QPVP beads (6 mg of dried beads, 15 mL solution), initial concentration of Cr(VI) ranged from 0.5 mg L^{-1} to 10 mg L^{-1}, along with the nonlinear fittings for Langmuir, Freundlich and D–R models. The linear fits are available as Supplementary Material Figure SM5. Table 4 shows the parameters determined from nonlinear and linear fittings corresponding to each adsorption model, along with the χ^2 and R^2 values. The parameters determined from the nonlinear fittings with the Langmuir, Freundlich and D–R models showed that the Langmuir model presented the best fitting quality, yielding q_{max} value of 18 mg g^{-1} and affinity constant of 124 L mol^{-1}. The linear fitting with Langmuir model had poor quality. The nonlinear and linear fittings obtained with Freundlich model converged to similar n and K_F values. Similarly to the adsorption isotherm of QPVP onto Alg beads (Fig. 1), the nonlinear fitting with D–R model converged only in the low C_e range (up to 0.5 mg L^{-1}). On the other hand, the linear fit for D–R model yielded q_{max} = 156 mg g^{-1} and E = 9.8 kJ mol^{-1}; this value for

Table 3
Contents of C, O, Ca and N (%) determined by means of XPS on Alg and Alg-QPVP beads surface.

	C1s (%)	O1s (%)	Ca2p (%)	N1s	Traces (Si)
Alg	53.3	43.2	1.8	0	1.7
Alg-QPVP	74.1	21.4	n.d.	4.0	0.5

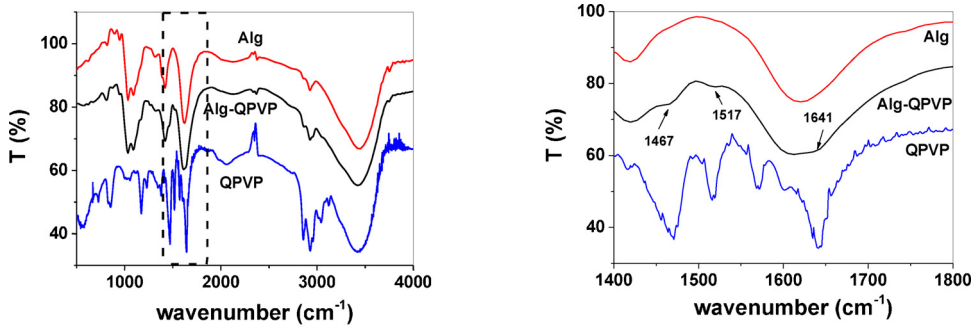

Fig. 2. FTIR spectra obtained for dried Alg and Alg-QPVP beads in the range of (a) 500 to 4000 cm^{-1} and (b) 1400 to 1800 cm^{-1}. (For interpretation of the references to colour in this figure legend, the reader is referred to the web version of this article.)

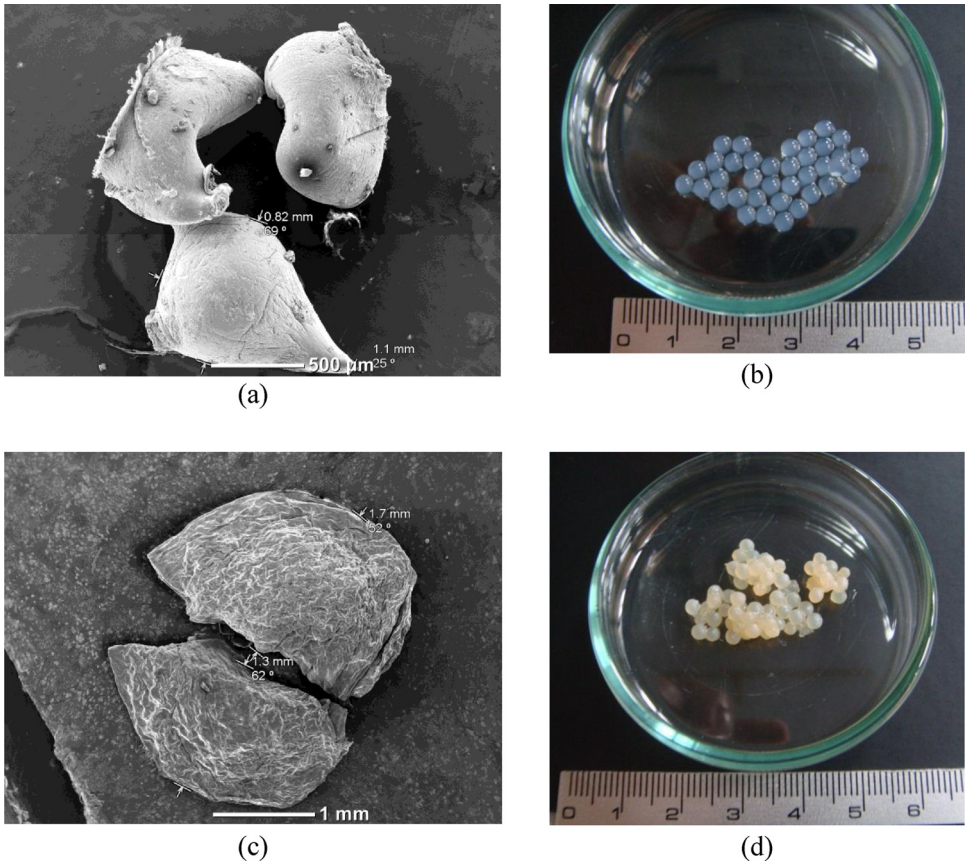

Fig. 3. SEM images of dried (a) Alg and (c) Alg-QPVP beads. Photographs of wet (b) Alg and (d) Alg-QPVP beads.

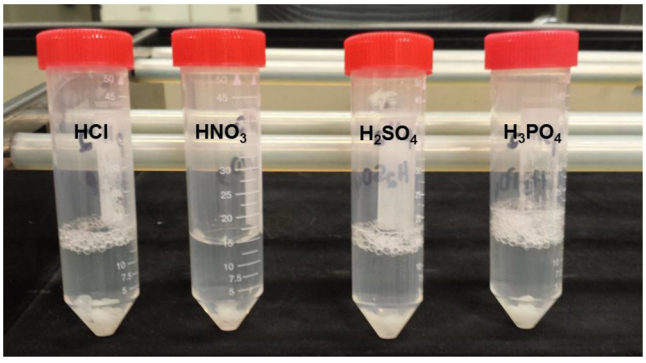

Fig. 4. Photograph of the vials containing Alg-QPVP beads after 30 min in contact with solutions of HNO_3, HCl, H_2SO_4 and H_3PO_4 (pH 2).

adsorption energy is consistent with the electrostatic interaction among Cr(VI) and QPVP cationic chains. For comparison, the adsorption of Cr (VI) onto barium ion cross-linked alginate beads was fitted by D–R model, yielding q_{max} and E values of 31 mg g^{-1} and 4.1 kJ mol^{-1}; the low magnitude of E was attributed to physical adsorption [22].

Table 5 comprises experimental parameters (pH, concentration range of Cr(VI), mass of adsorbent, volume of Cr(VI) solution) and q_{max} values reported for different adsorbents [9,12–15,22–28], considering both linear and nonlinear fittings, along with those obtained herein. In comparison to other biosorbents, the q_{max} value determined for Cr(VI) onto Alg-QPVP beads was on the order of magnitude of the q_{max} values reported for hybrid Alg beads [27,28]. However, the contact time necessary for Cr(VI) to achieve adsorption equilibrium onto Alg-QPVP beads was the shortest, and the concentration range of Cr(VI) was the smallest of all. These features are particularly important for a rapid and efficient removal of Cr(VI) from drinking water, in which the maximum allowed level is 0.1 mg L^{-1} (http://www.nsf.org/consumer-resources/water-quality/water-filters-testing-treatment/contaminant-testing-procedures).

3.3. Adsorption experiments in column system

For practical purposes, the potentiality of Alg-QPVP beads was tested in adsorption experiments using a fixed bed column system packed with 2 g of wet (i.e., 60 mg of dried) Alg-QPVP beads (bed depth of 12 cm), at 0.5 mL min^{-1} flow rate. The breakthrough curves (C_0 = 100 mg L^{-1} at pH 1) clearly show that the adsorption process is very fast (Fig. 6); the plateau is achieved after 18 min, indicating that Cr (VI) ions are adsorbed on the beads surface rather than in their interior. In order to gain insight about the dynamic behavior of the column, the experimental data were fitted to the Adams-Bohart and Thomas models [29].

Adams-Bohart model [30] is adequate for adsorption process where the adsorbent sites are mainly on the surface; it is generally applied to describe the initial part of the breakthrough curve. The equation and its linearized form are:

$$\frac{C_t}{C_0} = exp(K_{AB}C_0 t - K_{AB}N_0\frac{h}{v}) \quad (5)$$

$$\ln\left(\frac{C_t}{C_0}\right) = K_{AB}C_0 t - K_{AB}N_0\frac{h}{v} \quad (6)$$

where K_{AB} is the rate constant (L mg^{-1} min^{-1}), N_0 is the removal capacity (mg L^{-1}), h is the bed depth (cm) and v is the flow rate (mL min^{-1} cm^{-2}). The linear dependence of $\ln(C_t/C_0)$ on t yields the parameters K_{AB} and N_0.

Thomas model is adequate for constant flow rate and matches the Langmuir isotherm model and reversible adsorption process. The

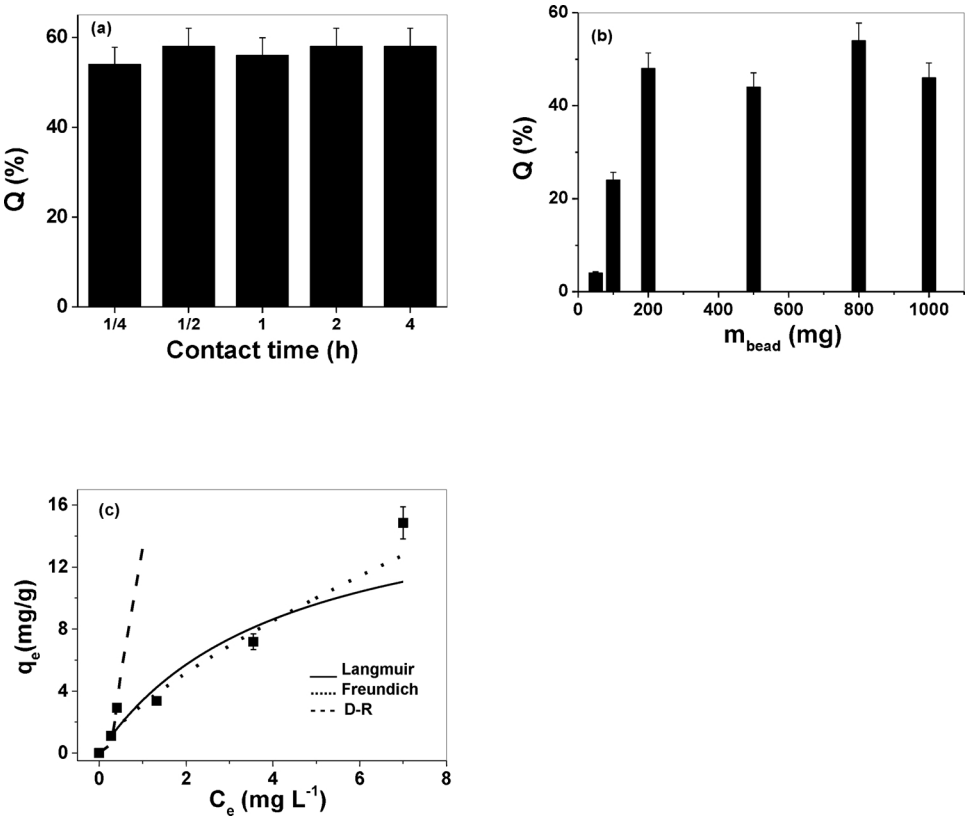

Fig. 5. The dependence of the *Q* values on the: (a) contact time of 400 mg wet Alg-QPVP beads in 15 mL standard solution of Cr(VI) at pH 2, at 1 mg L^{-1}, stirring at 300 rpm; (b) the mass of wet Alg-QPVP beads in contact with standard solution of Cr(VI) at pH 2, 1 mg L^{-1}, stirring at 300 rpm, for one hour; (c) Adsorption isotherm of Cr(VI) solution on Alg-QPVP beads (6 mg of dried beads, 15 mL) at pH 2, stirring at 300 rpm for 30 min, along with nonlinear fittings for Langmuir, Freundlich and D–R models. All experiments were performed at 24 ± 1 °C.

Table 4
Equilibrium adsorption of Cr(VI) onto Alg-QPVP beads. Parameters determined from nonlinear and linear fittings corresponding to each adsorption model, along with the χ^2 and R^2 values.

Nonlinear fitting		
Langmuir	Freundlich	D-R
q_{max} = 18 mg g^{-1} K_L = 0.2375 L mg^{-1}	n = 0.7227 $K_F = 3.1282\left(\frac{mg}{Lg}\right)/\left(\frac{mg}{Lg}\right)^{\frac{1}{n}}$	q_{max} = 332 mg g^{-1} E = 1.25 kJ mol^{-1}
χ^2 = 24.57	χ^2 = 16.91	χ^2 = 215
Linear fitting		
Langmuir	Freundlich	D-R
– –	n = 0.6776 $K_F = 3.4387\left(\frac{mg}{Lg}\right)/\left(\frac{mg}{Lg}\right)^{\frac{1}{n}}$	q_{max} = 156 mg g^{-1} E = 9.8 kJ mol^{-1}
–	R^2 = 0. 8821	R^2 = 0.8746

equation and its linearized form are:

$$\frac{C_t}{C_0} = \frac{1}{1 + exp\left[\frac{K_{Th}}{v} q_{max} m - K_{Th} C_0 t\right]} \quad (7)$$

$$\ln\left(\frac{C_0}{C_t} - 1\right) = -K_{Th} C_0 t + \frac{K_{Th} q_{max}\, m}{v} \quad (8)$$

where K_{Th} is the rate constant (L mg^{-1} min^{-1}), m is the mass of adsorbent, q_{max} is the maximal adsorption capacity (mg g^{-1}) and v is the flow rate (mL min^{-1}). The linear dependence of $\ln(C_0/C_t$ -1) on t yields the parameters K_{Th} and q.

The experimental breakthrough curve was fitted with nonlinear Adams-Bohart and Thomas models, as shown in Fig. 6a, whereas the corresponding linear fittings are presented as Supplementary Material SM6. Fig. 6b shows a photograph of 100 mg L^{-1} of Cr(VI) solution (1) before and (2) after passing through the column; the disappearance of yellow color after passing through the column clearly demonstrated the column high efficiency.

Table 6 comprises the parameters determined from nonlinear and linear fittings corresponding to each model, along with the χ^2 and R^2 values. The nonlinear and linear fittings with Adams-Bohart model converged with the experimental data only the first six minutes. For this initial stage the nonlinear and linear fitting parameters were similar. The K_{AB} value (~ 1.4×10^{-3} L mg^{-1} min^{-1}) indicated that the process is fast, and the N_0 value showed that the column should be saturated for C_0 of Cr(VI) higher than ~ 140 mg L^{-1}. Considering that the QPVP chains are mainly on the surface of Alg beads, the Cr(VI) might readily adsorb on the QPVP segments, making the process very fast. If the binding sites were in the interior of the beads, the Cr(VI) ions would take longer to reach the binding sites. The parameters determined from nonlinear fitting with Thomas model were slightly higher than those obtained with linear fitting. The K_{Th} value (~ 1.44×10^{-3} L mg^{-1} min^{-1}) was similar to that determined from Adams-Bohart. The q_{max} value (6.7 mg g^{-1}) was smaller than that estimated from the Langmuir model (18 mg g^{-1}) (Table 4) in the batch experiments, but it is expected due to the intrinsic characteristic of each adsorption process type. Similar trends were observed for the adsorption of Cr(VI) on PEI modified Alg beads [12].

The breakthrough curve of Cr(VI) (C_0 = 10 mg L^{-1} at pH 1) adsorption onto Alg-QPVP beads in fixed bed (bed depth of 12 cm, 2 g of wet beads = 60 mg of dried beads) column at constant flow rate of 0.5 mL min^{-1} is presented in Fig. 7a. The behavior for C_0 = 10 mg L^{-1} is quite different from that observed in Fig. 6 for C_0 = 100 mg L^{-1}. It seems that the effective contact with the QPVP binding sites was retarded due to the high dilution, and no change in the adsorption behavior was observed up to 25 min, resembling a steady state. For this reason, no model was applied to the experimental data. On the other hand, the desorption behavior was carefully investigated by loading 2 mL of a 0.2% (w m^{-1}) ascorbic acid (vitamin C) in 0.1 mol L^{-1} HCl in

Table 5
Experimental parameters (pH, concentration range of Cr(VI), mass of adsorbent (m_{ads}), volume of Cr(VI) solution, contact time), q_{max} values and the number of adsorbent reuse reported for different adsorbents and those obtained herein. (L) and (NL) stand for q_{max} determined from linear and nonlinear fittings.

Adsorbent	pH	Cr(VI) range (mg L^{-1})	m_{ads} (mg)	Vol (mL)	Contact time (min)	q_{max} (mg g^{-1})	Reuse
Alg-polydopa- PEI [13]	2	25-1000	20	20	1440	$524.7^{(NL)}$	5
Alg-PEI [12]	2	25-800	20	20	1440	$431.6^{(NL)}$	8
Carboxylated CNC-PEI [14]	3	10 - 300	5	50	250	$358.4^{(L)}$	5
Amine-corn stalks [15]	natural	100	1500[a]	50	60	$200^{(L)}$	–
Cellulose-amine copolymer [23]	2-3	200-500	100	50	240	$129^{(L)}$	3
Ba-Alg beads [22]	4	10-312	100	10	240	$31^{(L)}$	–
Activated carbon from *Cucumis melo* peel [24]	3	100 – 400	250	100	180	$98^{(L)}$	–
Alg-graphene [25]	4	1-200	1000[a]	–	1440	$72.5^{(NL)}$	10
PANI/bacterial polysaccharide [26]	3	25-125	100	100	50	$68.4^{(L)}$	–
Chitosan/CMC/Silica [9]	1-2	20-220	100–500	250	60	$16^{(L)}$	–
Alg-zirconium oxide composites [27]	5	10- 500	50	20	6000	$9.8^{(L)}$	3
Magnetic Alg beads [28]	5	100	100	50	100	$14.29^{(L)}$	–
This work	**2**	**0.5-10**	**6**	**15**	**30**	**$18^{(L)}$ $156^{(NL)}$**	**20**

[a] g L^{-1}.

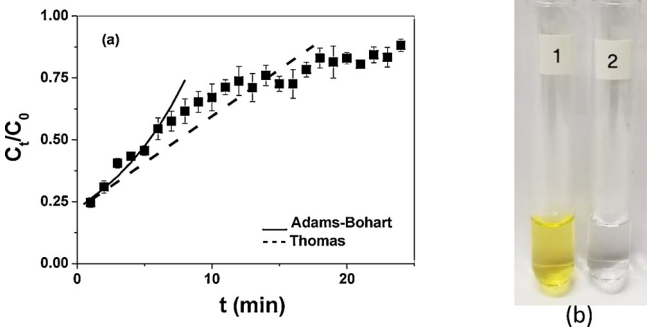

Fig. 6. (a) Breakthrough curve of Cr(VI) adsorption onto Alg-QPVP beads (60 mg of dried beads) in fixed bed column at constant flow rate of 0.5 mL min^{-1} C_0 = 100 mg L^{-1} Cr(VI) at pH 1, along with the nonlinear fittings to Adams-Bohart and Thomas models. (b) Photograph of 100 mg L^{-1} of Cr(VI) solution (1) before and (2) after passing through the column. (For interpretation of the references to colour in this figure legend, the reader is referred to the web version of this article.)

the reverse direction, at flow rate of 0.5 mL min^{-1}, and monitoring the Cr concentration in the eluate as a function of time, as shown in Fig. 7b. The desorption was promoted by the reduction of Cr(VI) by ascorbic acid, a low cost non-toxic biological reductant. The redox reaction involves the formation of Cr(III) and dehydroascorbic acid as products [31]:

$$Cr_2O_7^{2-} + 3\ C_6H_8O_6 + 8\ H^+ \rightarrow 2\ Cr^{3+} + 3\ C_6H_6O_6 + 7\ H_2O \quad (9)$$

Fig. 7b shows a fast desorption, since the Cr concentration in the eluate was high at the beginning and decreased exponentially with the time. The experimental data fitted well a first order kinetics (Supplementary Material SM7), yielding the rate constant of 0.1454 min^{-1}.

One should notice that although the use of ascorbic acid might be advantageous because it makes the reduction process very fast, polysaccharide based adsorbents have the ability to reduce Cr(VI) to Cr(III) [32]. The polysaccharide reducing ends (unmodified hemiacetal or hemiketal groups) are able to reduce the Cr(VI) to Cr(III) ions and to undergo oxidation into carboxylic acid. In the case of adsorbed Cr(VI) ions on QPVP-Alg, the reduction to Cr(III) took about eight hours.

3.4. Stability and regeneration

The adsorbent long-term stability aiming at repeated usage under flow are important parameters. For this reason, adsorption-desorption performance of the Alg-QPVP beads was evaluated under dynamic conditions. All experiments were performed at flow rate of 0.5 mL min^{-1} and the fixed bed column was packed with 2 g of wet Alg-QPVP beads (i.e., 60 mg dried basis, bed depth of 12 cm). First, the column was conditioned by loading 3 mL of 0.1 mol L^{-1} HNO_3 solution. Then 100 mg L^{-1} Cr(VI) solution at pH 1 was loaded. After 15 min the beads became yellow and the eluate came out colorless, similarly to Fig. 6b. In

Table 6
Adsorption of Cr(VI) ions onto Alg-QPVP beads in fixed bed column. Parameters determined from nonlinear and linear fittings corresponding to Adams-Bohart and Thomas models, along with the χ^2 and R^2 values.

Nonlinear fitting	
Adams-Bohart	Thomas
K_{AB} = 1.41 × 10^{-3} L mg^{-1} min^{-1} N_0 = 136 mg L^{-1} χ^2 = 22	K_{Th} = 1.47 10^{-3} L mg^{-1} min^{-1} q_{max} = 6.7 mg/g χ^2 = 0.2
Linear fitting	
Adams-Bohart	Thomas
K_{AB} = 1.48 × 10^{-3} L mg^{-1} min^{-1} N_0 = 147.5 mg L^{-1} R^2 = 0.9192	K_{Th} = 1.0 10^{-3} L mg^{-1} min^{-1} q_{max} = 3.6 mg/g R^2 = 0. 9296

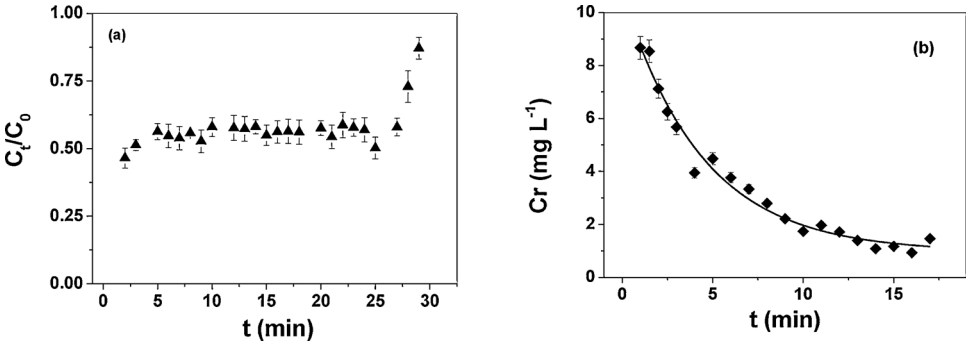

Fig. 7. (a) Breakthrough curve of Cr(VI) adsorption onto Alg-QPVP beads in fixed bed column at constant flow rate of 0.5 mL min^{-1} C_0 = 10 mg L^{-1} Cr(VI) at pH 1. The fixed bed column was packed with 2 g of wet Alg-QPVP beads (i.e., 60 mg dried basis, bed depth of 12 cm). (b) Concentration of eluted Cr after reaction with ascorbic acid as a function of time, the red line is an exponential fit with R^2 = 0.9783.

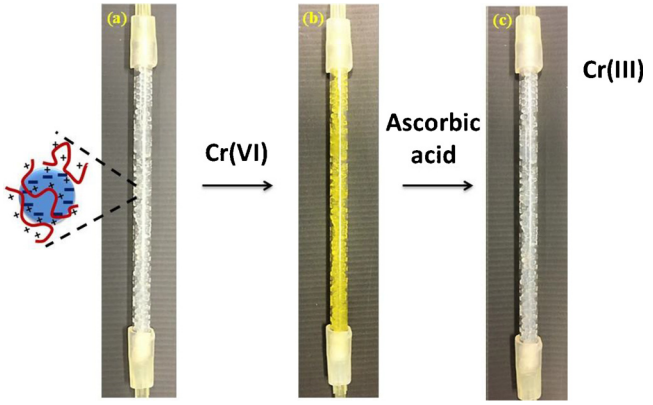

Fig. 8. Photographs of the Alg-QPVP beads column (a) before Cr(VI) loading, (b) after adsorption of Cr(VI) ions and (c) regenerated after redox reaction with ascorbic acid. (For interpretation of the references to colour in this figure legend, the reader is referred to the web version of this article.)

the sequence, 2 mL of a 0.2% (w m^{-1}) ascorbic acid in 0.1 mol L^{-1} HCl solution was loaded in the reverse direction. After 15 min the column recovered the original appearance and the eluate was colorless, evidencing the reduction of Cr(VI) to Cr(III) and efficient desorption. Then, the column was conditioned by loading 3 mL of 0.1 mol L^{-1} HNO_3 solution, for the next run. Reutilization of the Alg-QPVP beads was confirmed for at least 20 consecutive adsorption/desorption cycles, keeping the appropriate reproducibility (coefficient of variation < 6%) by taking into account the concentration of Cr(VI) in the solution after passing through the column. Thus, the regeneration of Cr(VI) loaded Alg-QPVP beads was efficiently achieved by the reaction among Cr(VI) and ascorbic acid, which yielded positively charged Cr(III) species, which undergo electrostatic repulsion towards the QPVP chains, favoring the desorption process. The regeneration of the Alg-QPVP beads column is schematically demonstrated in Fig. 8. The redox-based desorption with ascorbic acid was considered an advantage for Cr(VI) desorption when compared with ion-exchange-based desorption using alkaline solution (*e.g.*, pH from 9 to 12) [12], since the stability of the proposed Alg-QPVP beads is impaired at pH > 11.

For many practical applications, the adsorbent cost might be decisive. Considering the local prices of raw materials used to produce Alg-QPVP beads at laboratory scale, the cost to produce 1 g of Alg-QPVP beads was estimate as US$ 0.50. However, due to the possibility of at least 20 reuses without losing performance, the cost can be reduced to US$ 0.025 per gram.

4. Conclusions

Novel low-cost adsorbents were created by coating Alg beads with QPVP, a polycation that is easily synthesized. The adsorption of Cr(VI) from aqueous solution onto Alg-QPVP beads in batch and column systems was very fast (15 min). The maximum adsorption capacity of Cr (VI) on Alg-QPVP of 18 mg g^{-1} and high adsorption energy (9.8 kJ mol^{-1}) in the dilute range (Cr(VI) concentration less than 10 mg L^{-1}) clearly demonstrate the high affinity among adsorbent and Cr(VI) ions. The dynamic adsorption studies evidenced that the adsorption of Cr(VI) ions takes place on the QPVP binding sites located mainly on the beads surface, turning the process very fast. Twenty adsorption-desorption cycles were successfully achieved by using ascorbic acid as an environmentally friendly agent to reduce Cr(VI) to Cr(III). The proposed adsorption substrate can be considered a reliable alternative aiming towards Cr(VI) removal from aqueous solution.

Acknowledgements

Authors thank Lucas G. Sales de Oliveira for his help during the adsorption experiments of QPVP onto Alg beads and Dr. Jani Trygg for XPS measurements. Authors gratefully acknowledge financial support from Fundação de Amparo à Pesquisa do Estado de São Paulo (FAPESP; Grants 2015/06161-1 and 2015/25103-2) and from Conselho Nacional de Desenvolvimento Científico e Tecnológico (CNPq Grant 306848/2017-1).

Appendix A. Supplementary data

Supplementary material related to this article can be found, in the online version, at doi:https://doi.org/10.1016/j.colsurfa.2018.08.053.

References

[1] S. Sharma, A. Bhattacharya, Drinking water contamination and treatment techniques, Appl. Water Sci. 7 (2017) 1043–1067.
[2] F. Fu, Q. Wang, Removal of heavy metal ions from wastewaters: a review, J. Environ. Manage. 92 (2011) 407–418.
[3] G.T. Grant, E.R. Morris, D.A. Rees, P.J.C. Smith, D. Thom, Biological interactions between polysaccharides and divalent cations: the egg-box model, FEBS Lett. 32 (1973) (1973) 195–198.
[4] J. He, J.P. Chen, A comprehensive review on biosorption of heavy metals by algal biomass: materials, performances, chemistry, and modeling simulation tools, Bioresour. Technol. Rep. 160 (2014) 67–78.
[5] G.G. Arantes de Carvalho, S. Kondaveeti, D.F.S. Petri, A.M. Fioroto, L.G.R. Albuquerque, P.V. Oliveira, Evaluation of calcium alginate beads for Ce, La and Nd preconcentration from groundwater prior to ICP OES analysis, Talanta 161 (2016) 707–712.
[6] G.G. Arantes de Carvalho, D.F.S. Petri, P.V. Oliveira, Calcium alginate microparticles for rare earth elements preconcentration prior to ICP-MS measurements in fresh water, Anal. Methods (2018), https://doi.org/10.1039/c8ay01626g.
[7] A. Kabata-Pendias, A.B. Mukherjee, Trace Elements From Soil to Human, Springer-Verlag, Berlin Heidelberg, 2012.
[8] J. Zhang, M.D. Dong, S.K. Li, Cancer mortality in a Chinese population exposed to hexavalent chromium in water, J. Occup. Environ. Med. 39 (1997) 315–319.
[9] X. He, H. Xu, H. Li, Cr(VI) Removal from Aqueous Solution by Chitosan/Carboxylmethyl Cellulose/Silica Hybrid Membrane, World J. Eng. Technol. 3 (2015) 234–240.
[10] X.J. Hu, J.S. Wang, Y.G. Liu, X. Li, G.M. Zeng, Z.L. Bao, X.X. Zeng, A.W. Chen, F. Long, Adsorption of chromium (VI) by ethylenediamine-modified cross-linked magnetic chitosan resin: Isotherms, kinetics and thermodynamics, J. Hazard. Mater. 185 (2011) 306–314.
[11] Z. Li, T. Li, L. An, H. Liu, L. Gu, Z. Zhang, Preparation of chitosan/polycaprolactam nanofibrous filter paper and its greatly enhanced chromium(VI) adsorption, Colloids Surf. A: Physicochem. Eng. Aspects 494 (2016) 65–73.

[12] Y. Yan, Q. An, Z. Xiao, W. Zheng, S. Zhai, Flexible core-shell/bead-like alginate@PEI with exceptional adsorption capacity, recycling performance toward batch and column sorption of Cr(VI), Chem. Eng. J. 313 (2017) 475–486.
[13] Y. Yan, Q. An, Z. Xiao, S. Zhai, B. Zhai, Z. Shi, Interior multi-cavity/surface engineering of alginate hydrogels with polyethylenimine for highly efficient chromium removal in batch and continuous aqueous systems, J. Mater. Chem. A 5 (2017) 17073–17087.
[14] C. Liu, R.-N. Jin, X.K. Ouyang, Y.G. Wang, Adsorption behavior of carboxylated cellulose nanocrystal—polyethyleneimine composite for removal of Cr(VI) ions, Appl. Surf. Sci. 408 (2017) 77–87.
[15] S. Chen, Q. Yue, W. Zhou, Q. Li, X. Xu, Removal of Cr(VI) from aqueous solution using modified corn stalks: characteristic, equilibrium, kinetic and thermodynamic study, Chem. Eng. J. 168 (2011) 909–917.
[16] W. Cao, Z. Wang, H. Ao, B. Yuan, Removal of Cr(VI) by corn stalk based anion exchanger: the extent and rate of Cr(VI) reduction as side reaction, Colloids Surf. A: Physicochem. Eng. Aspects 539 (2018) 424–432.
[17] L.S. Blachechen, P. Fardim, D.F.S. Petri, Multifunctional cellulose beads and their interaction with gram positive Bacteria, Biomacromolecules 15 (2014) 3440–3448.
[18] L.S. Blachechen, J. Amim Jr, N. Lincopan, D.F.S. Petri, Carboxymethylcellulose acetate butyrate/poly(4-vinyl-N-pentyl pyridinium bromide) blends as antimicrobial coatings, Exp. Polym. Lett. 9 (2015) 790–798.
[19] K.Y. Foo, B.H. Hameed, Insights into the modeling of adsorption isotherm systems, Chem. Eng. J. 156 (2010) 2–10.
[20] H.N. Tran, S.J. You, A. Hosseini-Bandegharaei, H.-P. Chao, Mistakes and inconsistencies regarding adsorption of contaminants from aqueous solutions: a critical review, Water Res. 120 (2017) 88–116.
[21] R.A. Silva, M.A. Urzua, D.F.S. Petri, Lysozyme binding to poly(4-vinyl-*N*-alkylpyridinium bromide), J. Colloid Interf. Sci. 330 (2009) 310–316.
[22] S. Uzaşçi, F. Tezcan, F.B. Erim, Removal of hexavalent chromium from aqueous solution by barium ion cross-linked alginate beads, Int. J. Environ. Sci. Technol. (Tehran) 11 (2014) 1861–1868.
[23] X. Xu, B.Y. Gao, X. Tang, Q.Y. Yue, Q.Q. Zhong, Q. Li, Characteristics of cellulosic amine-crosslinked copolymer and its sorption properties for Cr(VI) from aqueous solutions, J. Hazard. Mater. 187 (2011) 420–426.
[24] M. Manjuladevi, R. Anitha, S. Manonmani, Kinetic study on adsorption of Cr(VI), Ni (II), Cd(II) and Pb(II) ions from aqueous solutions using activated carbon prepared from Cucumis melo peel, Appl. Water Sci. 8 (2018) 36–42.
[25] Y. Zhuang, F. Yu, H. Chen, J. Zheng, J. Ma, J. Chen, Alginate/graphene double-network nanocomposite hydrogel beads with low-swelling, enhanced mechanical properties, and enhanced adsorption capacity, J. Mater. Chem. A 4 (2016) 10885–10892.
[26] V. Janaki, M.N. Shin, S.H. Kim, K.J. Lee, M. Cho, A.K. Ramasamy, B.T. Oh, K.K. Seralathan, Application of polyaniline/bacterial extracelular polysaccharide nanocomposite for removal and detoxification of Cr(VI), Cellulose 21 (2014) 463–472.
[27] R. Kumar, S.J. Kim, K.H. Kim, S.H. Lee, H.S. Park, B.H. Jeon, Removal of hazardous hexavalent chromium from aqueous phase using zirconium oxide-immobilized alginate beads, Appl. Geochem. 88(A (2018) 113–121.
[28] V. Gopalakannana, N. Viswanathan, Synthesis of magnetic alginate hybrid beads for efficient chromium (VI) removal, Int. J. Biol. Macromol. 72 (2015) 862–867.
[29] M. Trgo, N.V. Medvidović, J. Perić, Application of mathematical empirical models to dynamic removal of lead on natural zeolite clinoptilolite in a fixed bed column, Indian J. Chem. Technol. 28 (2011) 123–131.
[30] Bohart G.S, E.Q. Adams, Behavior of charcoal towards chlorine, J. Chem. Soc. 42 (1920) 523–529.
[31] X.R. Xu, H.B. Li, X.Y. Li, J.D. Gu, Reduction of hexavalent chromium by ascorbic acid in aqueous solutions, Chemosphere 57 (2004) 609–613.
[32] Y. Zhang, S. Lin, J. Qiao, Y. Ju, M. Zhang, M. Cai, D. Deng, D.D. Dionysiou, Malic acid-enhanced chitosan hydrogel beads (mCHBs) for the removal of Cr(VI) and Cu (II) from aqueous solution, Chem. Eng. J. 353 (2018) 225–236 http://www.nsf.org/consumer-resources/water-quality/water-filters-testing-treatment/contaminant-testing-procedures (accessed 30 June 2018).